Docking of Noncompetitive Inhibitors into Dengue Virus Type 2 Protease: Understanding the Interactions with Allosteric Binding Sites

Rozana Othman,[†] Tan Siew Kiat,[§] Norzulaani Khalid,[||] Rohana Yusof,[‡] E. Irene Newhouse,[#] James S. Newhouse,[▽] Masqudul Alam,[○] and Noorsaadah Abdul Rahman*[,⊥]

Pharmacy Department and Department of Molecular Medicine, Faculty of Medicine and Institute of Biological Sciences and Chemistry Department, Faculty of Science, Universiti Malaya, 50603 Kuala Lumpur, Malaysia, Sunway University College, Bandar Sunway, 46150 Petaling Jaya, Malaysia, Advanced Studies in Genomics, Proteomics and Bioinformatics, University of Hawaii at Manoa, 2565 McCarthy Mall, Keller 319, Honolulu, Hawaii 96822, Maui High Performance Computing Center, 550 Lipoa Parkway, Kihei, Hawaii 96753, and Department of Microbiology, University of Hawaii at Manoa, 2538 McCarthy Mall, Snyder 111, Honolulu, Hawaii 96822

Received October 26, 2007

A group of flavanones and their chalcones, isolated from *Boesenbergia rotunda* L., were previously reported to show varying degrees of noncompetitive inhibitory activities toward Dengue virus type 2 (Den2) protease. Results obtained from automated docking studies are in agreement with experimental data in which the ligands were shown to bind to sites other than the active site of the protease. The calculated K_i values are very small, indicating that the ligands bind quite well to the allosteric binding site. Greater inhibition by pinostrobin, compared to the other compounds, can be explained by H-bonding interaction with the backbone carbonyl of Lys74, which is bonded to Asp75 (one of the catalytic triad residues). In addition, structure−activity relationship analysis yields structural information that may be useful for designing more effective therapeutic drugs against dengue virus infections.

INTRODUCTION

Dengue virus belongs to the *Flaviviridae* family and is a widespread human pathogen that can cause diseases ranging from a harmless flulike illness to a severe hemorrhagic fever with high mortality rate, especially in children.[1] Dengue infections place some 2.5 billion people (or 40% of the world population) at risk and are a significant cause of mortality, especially in the tropical and subtropical regions,[2] and have been on the rise globally in recent years. In Malaysia, the Health Ministry's Parliamentary Secretary reported that dengue fever killed 44 people in the first four months of 2007, and a record number of suspected dengue cases occurred in 2007, with 900 cases in the first week of June alone. This is an increase of more than 100% compared to the same period of 2006.[3] Management of dengue fever is largely supportive, while its more severe hemorrhagic manifestation may require blood transfusions.

The most prevalent of the four dengue serotypes is Dengue virus type 2 (Den2), which contains a single-stranded RNA of positive polarity. The RNA genome codes for a single polyprotein precursor of 3,391 amino acids, arranged in the order C-prM-E-NS1-NS2A-NS2B-NS3-NS4A-NS4B-NS5, comprising three structural and seven nonstructural proteins.[4] Flavivirus replication is dependent upon the correct cleavage of this polypeptide and requires both host cell proteases and the virus-encoded, two-component protease, NS2B-NS3.[5,6] NS3 contains a trypsin-like serine proteinase domain of 180 amino acid residues at its N-terminal, suggesting its role as the putative viral protease.[7,8] Analysis of virus sequence alignments indicates the catalytic triad of Den2 protease is His51, Asp75, and Ser135.[9] The N-termini of several nonstructural proteins are produced through cleavage by NS2B-NS3 at dibasic sites. Optimal catalytic activity of NS3 depends on the presence of NS2B. Biochemical studies and deletion analyses have mapped the required region on the NS2B to a central, hydrophilic 40 amino acid domain (Lys54-Glu93) in an otherwise relatively hydrophobic protein.[6,10,11] Hence, the NS2B-NS3 protease complex serves as a target in the development of antiviral drugs.

In spite of the efforts of many research groups,[12–17] no vaccines or antiviral drugs are currently available against dengue viral infections.[18] Thus, there is an immense ongoing interest in developing new antiviral therapeutic agents to fight diseases caused by dengue viruses.

Many research groups worldwide search for antiviral therapeutic agents from natural products. Nevertheless, this approach continues to furnish investigators with new and interesting findings. Several compounds from *Boesenbergia rotunda* (L.) Mansf. Kulturpfl. have shown noncompetitive inhibitory activity against the ability of Den2 protease to cleave fluorogenic peptide substrates.[12,19] *Boesenbergia rotunda* (L.) belongs to the ginger family (Zingiberaceae)

* Corresponding author phone: +603 7967 4254; fax: +603 7967 4193; e-mail: noorsaadah@um.edu.my.
[†] Pharmacy Department, Faculty of Medicine, Universiti Malaya.
[§] Sunway University College.
[||] Institute of Biological Sciences, Faculty of Science, Universiti Malaya.
[‡] Department of Molecular Medicine, Faculty of Medicine, Universiti Malaya.
[#] Advanced Studies in Genomics, Proteomics and Bioinformatics, University of Hawaii at Manoa.
[▽] Maui High Performance Computing Center.
[○] Department of Microbiology, University of Hawaii at Manoa.
[⊥] Chemistry Department, Faculty of Science, Universiti Malaya.

10.1021/ci700388k CCC: $40.75
Published on Web 07/26/2008

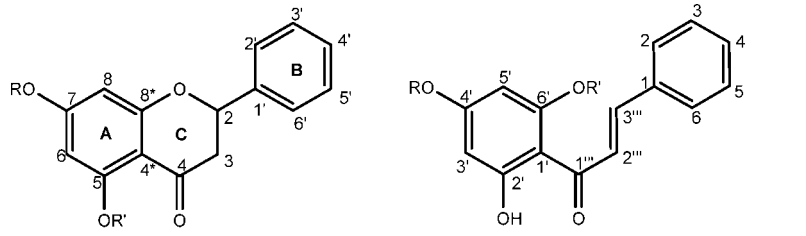

R = OMe, R' = OH : Pinostrobin (**1**)
R = OH, R' = OH : Pinocembrin (**2**)
R = OH, R' = OMe : Alpinetin (**3**)

R = OMe, R' = OH : Pinostrobin chalcone (**4**)
R = OH, R' = OH : Pinocembrin chalcone (**5**)
R = OH, R' = OMe : Cardamonin (**6**)

Figure 1. Structures of the compounds extracted from *Boesenbergia rotunda* L.

and is a spice commonly used in Southeast Asia, especially in Malaysia and Indonesia. Some reports have indicated it has medicinal properties, and it has been used traditionally, mainly for problems and diseases of women, such as in postpartum protective medication, treatment for rheumatism, and as a tonic/lotion.[20] Scientific reports on the anti-inflammatory and anti-HIV activities of extracts from this plant have also been published.[21–23]

In this study, we report automated docking studies performed on the compounds which exhibited noncompetitive inhibitory activities toward NS2B-NS3 of Den2, using AutoDock 3.0.5 and Glide[24] software. The subjects of this study are the flavanones: pinostrobin, pinocembrin, and alpinetin and their chalcone derivatives: pinostrobin chalcone, pinocembrin chalcone, and cardamonin, respectively (Figure 1). The aim of this study is to understand the interactions involved in the binding of these compounds (referred to as ligands hereafter) to NS2B-NS3 of Den2 via computational docking methods and to gain insights into the experimental inhibition pattern.[19] It is hoped that information from this study will provide further understanding of the mechanism of inhibition of Den2 protease and enable the design of antiviral drugs which inhibit dengue virus replication.

EXPERIMENTAL METHODS

Purification and Screening of Ligands for Inhibition Activities. The purification techniques used to isolate the ligands involved in this study and the methods used in their biological screening for inhibition of proteolytic activity of Den2 NS2B-NS3 have been reported.[12,19] The fluorogenic substrate used in these studies was Boc-Gly-Arg-Arg-MCA. Den2 NS3 protease has been shown to cleave this substrate.

Building Protein and Ligand Structures for Computational Docking Experiments. The three-dimensional structure of Den2 NS2B-NS3 was retrieved from the Protein Data Bank (http://www.rcsb.org/pdb; accession code 2FOM). Chlorine atoms, water, and glycerol molecules were removed. Crystal coordinates of the flavanones were obtained from the Cambridge Crystallographic Data Centre and related publications.[25–27] Structures of the chalcones were built from the flavanones using Hyperchem Pro 6.0 software (Hypercube Inc.). Ligand structures were minimized with Hyperchem using the steepest descent and conjugate gradient methods (termination conditions set to a maximum of 500 cycles or 0.1 kcal/Å mol rms gradient).

Automated Rigid-Ligand Docking. Docking files were prepared using AutoDock Tools v.1.4 software.[28] For the protein molecule, polar hydrogen atoms were added and nonpolar hydrogen atoms were merged and Kollman charges and solvation parameters were assigned by default. For the ligands, Gasteiger charges were added, nonpolar hydrogen atoms were merged, and all bonds were made nonrotatable. All docking calculations were done with the AutoDock 3.0.5 software package using the Lamarckian genetic algorithm (LGA).[29] A population size of 150 and 250,000 energy evaluations were used for 100 search runs. The grid box, with grid spacing of 0.375 Å and dimension of 128 × 100 × 116 points along the x, y, and z axes, was centered on the macromolecule. After the docking searches were completed, clustering histogram analyses were performed, based on an rmsd (root-mean-square deviation) of not more than 1.0 Å. The conformation with the lowest docked energy was chosen from the most populated cluster and put through the next stage.

Automated Flexible-Ligand Docking. The methods involved were similar to the above, except that in ligand file preparation, torsional degrees of freedom were defined by allowing rotatable bonds to remain flexible. In addition, the grid box size was reduced to points, centered on the ligand. The number of energy evaluation was increased to 10 million. The conformations from the docking experiments were analyzed using Viewerlite 4.2 (http://www.accelrys.com), which also identified the H-bonding and van der Waals interactions between the protease and the ligands. LIGPLOT[30] was used to determine residues involved in hydrophobic interactions with the ligands. The HBPLUS[31] program in LIGPLOT calculates (by default) nonbonded/hydrophobic contacts, with cutoff in the range of 2.9−4.3 Å. The LIGPLOT algorithm[30] reads the three-dimensional (3D) structure of the ligands from the PDB files, together with the protein residues, and 'unrolls' each object about its rotatable bonds, flattening them out onto the 2D page.

Electrostatic Potential Map. Hyperchem Pro 6.0 was used to calculate single point energy of the ligands with the most favorable conformations using the semiempirical AM1 method. The electrostatic potentials of the ligands were then displayed as contour maps plotted in the form of 3-dimensional isosurfaces using Hyperchem. By default, Mulliken charges were used in the calculations to obtain the electrostatic potentials.

Glide Docking. The protein (PDB file as above) was prepared using the Protein Preparation Wizard of Schroedinger Suite 2007 (Schroedinger, Inc.). The suite's Site Map package was used to identify the potential binding sites; the noncompetitive site was selected for input into the Glide Receptor Grid Generation utility. The ligands were prepared either from sdf files found in the NCI database[32] or modified from similar compounds using the builder in the Maestro package of Schroedinger Suite 2007 and optimized using a

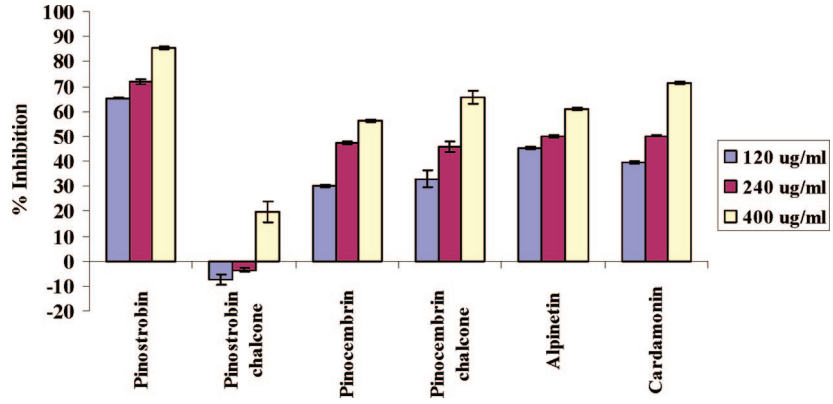

Figure 2. Percentage inhibition of DEN-2 NS2B/NS3 cleavage of substrate by ligands extracted from *Boesenbergia rotunda* L.[11,18] The standard 100 μL reaction mixtures comprised of 100 μM fluorogenic peptide subtrate Boc-Gly-Arg-Arg-MCA, 2 μM DEN-2 protease complex and with or without ligands of varying concentrations, buffered at pH 8.5 by 200 mM Tris-HCl. Each ligand was assayed at three different concentrations; 120 μg mL^{-1}, 240 μg mL^{-1}, and 400 μg mL^{-1}. Each test was done in quadruplicate. Four readings were taken—each at a time interval of 5 s per sample, and the three most consistent readings (% standard deviation <5%) were accepted.

Table 1. Automated Flexible-Ligand-Protein Docking Results Calculated Using AutoDock 3.0.5[a]

ligand	pinostrobin	cardamonin	alpinetin	pinocembrin chalcone	pinocembrin	pinostrobin chalcone
experimental IC_{50} (μg/mL)[18]	90.48	235.86	242.76	273.10	286.90	-
min. estimated free energy of binding, ΔG_{bind} (kcal/mol)	−8.30	−7.55	−8.84	−7.59	−9.25	−7.79
min. docked energy, E_{dock} (kcal/mol)	−8.82	−9.04	−9.45	−8.85	−9.57	−8.71
estimated inhibition constant, K_i (μM)	0.83	2.92	0.33	2.71	0.17	1.95
final intermolecular energy, ΔG_{inter} (kcal/mol)	−8.92	−8.80	−9.46	−8.53	−9.56	−9.03
final internal energy of ligand, ΔG_{intra} (kcal/mol)	+0.10	−0.25	+0.02	−0.32	0.00	+0.33
torsional free energy, ΔG_{tors} (kcal/mol)	+0.62	+1.25	+0.62	+0.93	+0.31	+1.25
rmsd (from ref structure) (Å)	0.61	3.15	0.60	2.05	0.88	4.60

[a] The IC_{50} values were obtained from experiments performed by Tan (2005).[18] The ligands are arranged in decreasing inhibition activity (increasing IC_{50} values) from left to right of the table. Estimated energy and K_i values shown were obtained from flexible docking of each ligand conformation which was initially the most favorable conformation obtained from rigid docking procedures (refer to the Experimental Methods section).

version of MacroModel also included. They underwent preparation using the Ligand Preparation utility of Schroedinger Suite 2007. The defaults, which were used, are set to generate states at pH 7 ± 2 and a maximum of 32 tautomers and stereoisomers, retaining specified chiralities, using the OPLS 2005 force field.[33] The outputs from Receptor Grid generation and Ligand Preparation are the inputs to Glide, which was run with standard precision (default settings), flexible docking, permitting 5- and 6-membered ring conformational interchange. Glide uses a grid approximation for the binding site, and an all-atom treatment of the ligands. Initial rough, rigid posing is followed by flexible energy minimization with an OPLS force field. The best poses are further refined using Monte Carlo methods. The output file is produced with best-scoring poses first and analyzed with Maestro's Pose Viewer utility.

RESULTS

Noncompetitive Inhibition of Den2 NS2B-NS3. Figure 2 shows the percentage of inhibition by the ligands, tested at three different concentrations. Results indicated pinostrobin to be the most active inhibitor, with up to 85.4% inhibition at 400 μg mL^{-1}, while its chalcone derivative, pinostrobin chalcone, did not exhibit any activity. However, in the other two cases, the chalcones were more active than their corresponding flavanones.

Tan et al. (2006) recently reported the noncompetitive inhibitory activities of some of these ligands.[12] The IC_{50} (ligand concentration at 50% inhibition) values are shown in Table 1, arranged in decreasing activity from left to right. The IC_{50} value of pinostrobin (90.48 μg mL^{-1}) is 2.6−3-fold smaller than the other ligands, indicating that it is the most active noncompetitive inhibitor.

Predicted Free Energy of Binding, Docking Energy, and K_i values. AutoDock was recently reported to be the most popular docking program.[34] Its high accuracy and versatility have expanded its use. In this study, rigid-ligand docking was initially performed using energetically optimized ligands at different potential binding sites of the whole protein (blind docking), since this reduces the time for the simulation to complete. Hetényi et al. (2002)[35] reported Autodock to be able to select the correct protein−ligand complexes, based on energy, without prior knowledge of the binding site (blind docking). Autodock has been proven to be efficient and robust in finding the binding pockets and binding orientations of the ligands, whether they are rigid (up to at least 30 heavy atoms) or flexible. As the ligands involved in this study are noncompetitive inhibitors, it was anticipated that they would dock to sites other than the active, requiring blind docking. SiteMap, part of the Schroedinger Suite 2007 (see Experimental Methods), identified largely the same noncompetitive binding site as Autodock. Glide[24] uses a ChemScore-derived algorithm to rank ligand binding; the more negative the score, the stronger the binding. The Glide scores are listed in Table 2.

Table 2. Automated Flexible, Extra-Precision-Ligand-Protein Docking Results Calculated Using Glide

ligand	pinostrobin	cardamonin	alpinetin	pinocembrin	pinocembrin chalcone	pinostrobin chalcone
Glide score	−7.14	−6.39	−6.86	−6.92	−5.55	−6.45

Table 3. Results of Rigid and Flexible Ligand Docking (AutoDock)[a]

		no. of free torsions		min. estimated ΔG_{bind} (kcal/mol)		final E_{dock} (kcal/mol)	
compounds	no. of atoms	rigid	flexible	rigid	flexible	rigid	flexible
pinostrobin	34	0	3	−8.23	−8.30	−8.23	−8.82
pinocembrin	31	0	3	−8.63	−9.25	−8.63	−9.57
alpinetin	34	0	3	−9.17	−8.84	−9.17	−9.45
pinostrobin chalcone	34	0	6	−7.74	−7.79	−7.74	−8.71
pinocembrin chalcone	31	0	6	−7.40	−7.59	−7.40	−8.85
cardamonin	34	0	6	−8.00	−7.55	−8.00	−9.04

[a] The energy values shown were obtained from flexible docking of each ligand conformation which initially was the most favorable conformation obtained from rigid docking procedures (refer to the Materials and Methods section).

Once the binding site for noncompetitive inhibition was identified, flexible-ligand docking was carried out at this site using Autodock. For this, a grid box of 60 × 60 × 60 number of points (grid spacing of 0.375 Å) was built around the binding region. Table 3 shows the calculated docking energy (E_{dock}) and free energy of binding (ΔG_{bind}) of both the rigid and flexible-ligand docking simulations. On the whole, energy values obtained from flexible docking were lower than those from rigid docking. Allowing the bonds in the ligands to rotate generated different ligand conformations, enabling more refined search for preferred binding sites.

The calculated energies and K_i (inhibitory constant) values do not follow the pattern of activity-ranking according to the observed IC_{50} values. Pinostrobin, the most active inhibitor, had the best Glide score. The remaining four inhibitors all had IC_{50} values between 200 and 300 μg mL^{-1}, so one might expect docking computations to be unable to discriminate between them. This highlights the challenge associated with scoring compound conformations and accurately predicting activity ranking using computational modeling techniques. Enthalpic and entropic effects drive ligand-binding processes, and either of these effects can dominate specific interactions.[36] However, if binding induces conformational changes in the protein, as often occurs in enzymatic interactions, using rigid binding sites limits the predictive ability to link experimental activity-ranking with calculated scoring functions.

In general, the estimated ΔG_{bind} for the flavanones obtained in this study were lower than those of their chalcone derivatives (Table 1). This is mainly because the chalcones have more rotatable bonds, increasing the torsional free energy (ΔG_{tor}) and lowering binding affinity (higher K_i values). On the other hand, the calculated K_i values for all the ligands are reasonably small (within the μM range), indicating the formation of stable enzyme−inhibitor complexes. Quantitative explanation of the experimental inhibitory activity of the ligands toward substrate-binding by the protease requires further structural insights.

Binding Site and Ligand Conformations. As expected, the automated docking experiments showed that all the ligands studied did not bind to the active site of the protease. Surprisingly, however, the binding site for these ligands was confined to a specific region of the protease (Figure 3a,b). The shape of the binding site can be divided into three parts (Figure 3b): the left region constitutes a hydrophobic hole which accommodates the aromatic rings of the ligands; the middle allows placement of flavanone ring C or the chains carrying the enone groups of the chalcones, enabling these ligands to interact with the surrounding residues; and the region on the right, bigger than the other two, allows more varied orientations of the ligands' pharmacophores. Presumably, the shape of the binding site complements the shapes of the ligands. Figure 3c,d shows the superimposition of the conformations of the flavanones and chalcones, respectively, at the binding sites computed with Autodock. Of the flavanones, pinocembrin and alpinetin take up similar poses. However, although pinostrobin lies on an axis similar to the other two ligands, it is oriented in the opposite direction, so that the phenyl ring projects into the region on the right side of the binding site.

Figure 3e shows the superposition of all six ligand conformations computed with Glide. Unlike Autodock, pinostrobin's orientation using Glide is similar to that of the other flavonoids. Like Autodock, pinostrobin chalcone binds differently from the five other ligands. The conformational difference between pinostrobin and the other flavanones obtained from Autodock is more clearly shown in Figure 4a−c which illustrates the three-dimensional (3D) isosurface plots of the electrostatic potential of the ligands. Similar plots were observed for alpinetin and pinocembrin, but the potential map for pinostrobin (colored green to indicate neutral to positive potential) is more elongated due to the presence of a methoxy group on ring A. Furthermore, the negative potentials (magenta) due to the carbonyl and hydroxyl groups on ring C and ring A, respectively, point toward the back of the plane of the model, while that due to the ether group on ring C points more toward the front of the plane of the model. The reverse was observed with alpinetin and pinocembrin. These observations infer the different chemical environment requirement of the binding site for docking of pinostrobin compared to alpinetin and pinocembrin. For the chalcones (Figure 4d−f), the shapes of the 3D isosurface plots of the electrostatic potential were different for each ligand. This could be attributable to the higher flexibility of the enone chains. This finding may also explain the requirement of a different (chemical) environment of the binding site by the ligands, hence the different orientations adopted by the ligands in the binding site.

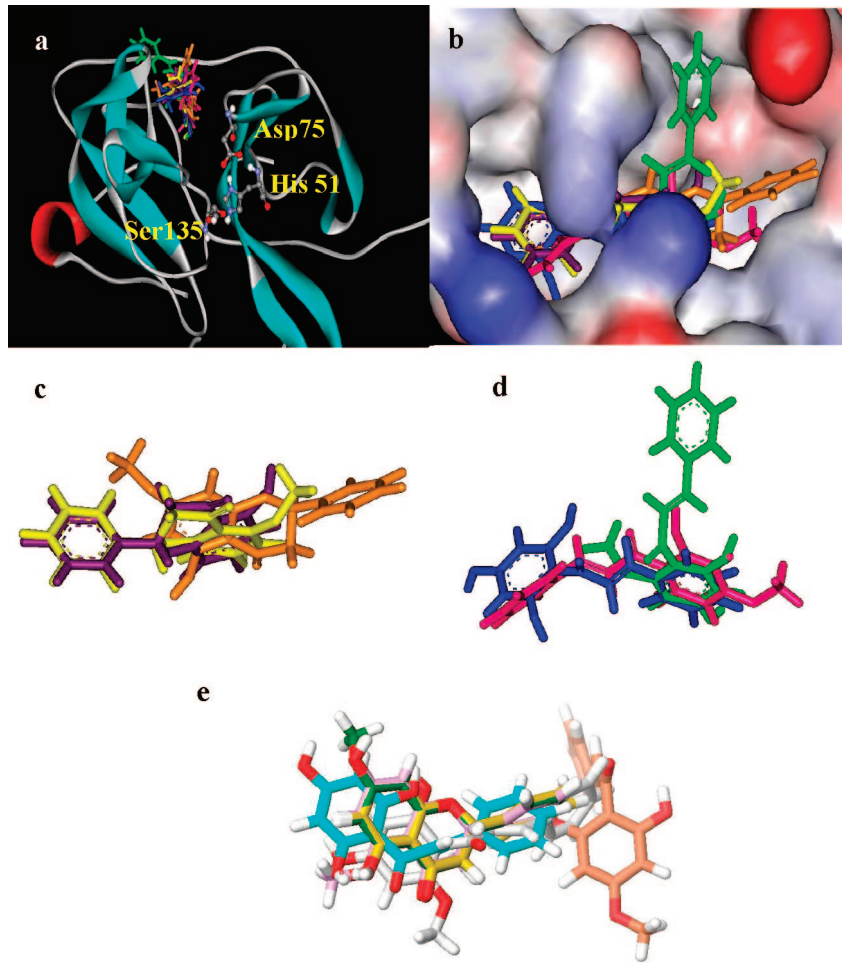

Figure 3. Computer generated models illustrating the superimposition of the flavanones, pinostrobin (orange), pinocembrin (purple), and alpinetin (yellow), and the chalcones, pinostrobin chalcone (pink), pinocembrin chalcone (blue), and cardamonin (green), at the binding site. The ligands are shown as sticks. (**a**) All the ligands are superimposed at the binding site. DEN-2 protease is represented as ribbons. The catalytic triads are labeled as His51, Asp75, and Ser135 and are shown as balls and sticks. (**b**) Connolly surface representation of the binding site colored according to electrostatic potential spectrum. (**c**) Superimposition of the flavanone poses as found in the binding site. (**d**) Superimposition of the chalcone poses as found in the binding site. (**e**) Glide poses of all ligands. Note that, as with Autodock, pinostrobin chalcone binds quite differently. The orange molecule is pinostrobin chalcone.

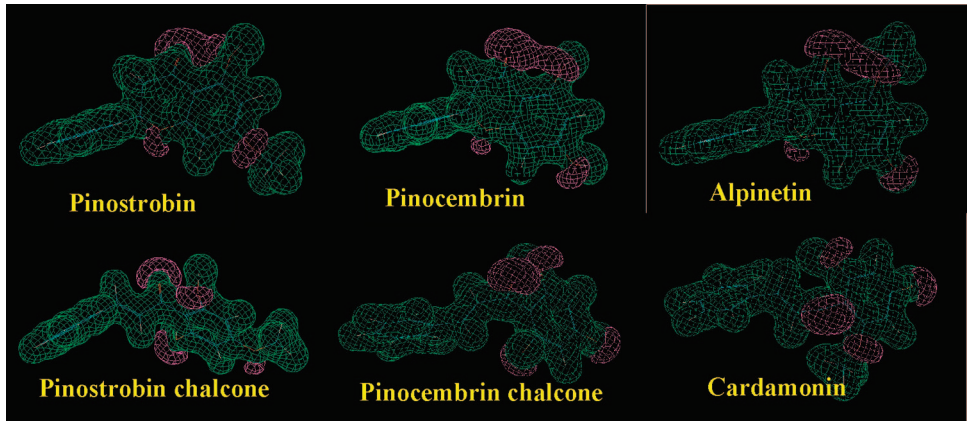

Figure 4. 3D isosurface plots of the electrostatic potentials of the ligands, using Hyperchem Pro 6.0 software. Green surfaces indicate neutral to positive potentials, while magenta surfaces indicate negative potentials.

DISCUSSION

Although both docking programs identified largely the same binding site, and docked pinostrobin chalcone differently from the other ligands, the details of the best poses from the two programs were different. Autodock's scoring appears to be more heavily tilted toward maximizing the number of hydrogen bonds than Glide. Glide was able to identify the best inhibitor but not the worst.

Binding Interactions. *Pinostrobin.* As shown in Table 1, pinostrobin showed the highest inhibition among all the ligands screened, with an IC_{50} value of 90.48 μg mL^{-1}, while pinostrobin chalcone was found to be inactive. Figure 5a,b

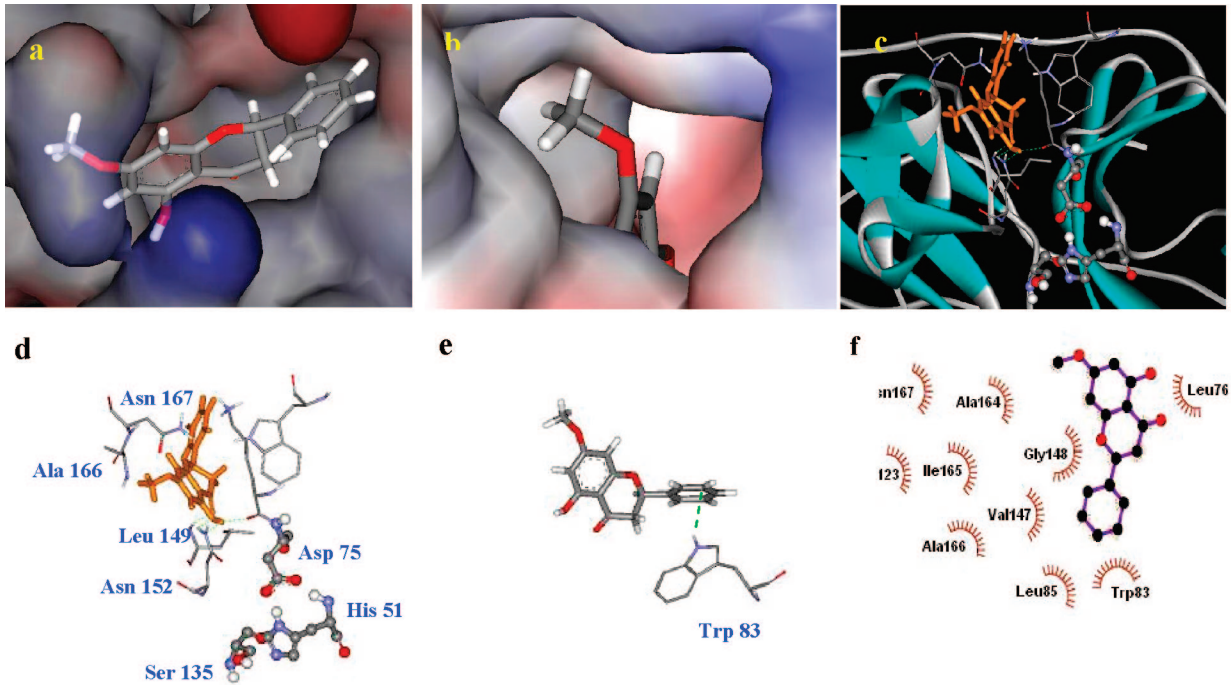

Figure 5. (**a**) Transparent Connolly surface representation of pinostrobin at the binding site. (**b**) View of pinostrobin in the binding site from a different angle. (**c**) View of pinostrobin (orange) at the binding site of Den2 protease (ribbons). Residues interacting with the ligand are shown as sticks. Catalytic triads are shown as balls and sticks. (**d**) Simplified view of pinostrobin interacting with surrounding residues. Residues labeled in green interact with the ligand via H-bonds, while those in red interact via van der Waals contacts. The catalytic triads are labeled in black. (**e**) Nonclassical H-bonding between Trp83 and phenyl ring B of pinostrobin. (**f**) 2D schematic diagram of residues in the binding site which exhibit hydrophobic interactions with pinostrobin, obtained using the Ligplot program. Keys for the plot are the following: (blue ball-purple stick-black ball) ligand bond; (His51 with curved railroad-like ties) nonligand residue involved in hydrophobic contact; and (black ball with railroad-like ties) corresponding atom involved in hydrophobic contact.

illustrated the binding site for pinostrobin. The shape of the binding pocket was observed to complement the shape (pose) of the ligand. The phenyl ring is protruded out toward the surface of the protein, while the rest of the molecule was embedded into the inner part of the protein. The surrounding residues involved in hydrogen bonding interactions with pinostrobin were Lys74, Leu149, and Asn152. The H-bonding interaction with Lys74 (Figure 5c,d) was not observed with the other flavanones and chalcones studied. The interaction between the hydroxyl H atom on ring A of pinostrobin with the backbone carbonyl O atom of Lys74 could account for the relatively high inhibition activity of pinostrobin. Since Lys74 is directly bonded to Asp75, the formation of H-bond between Lys74 and pinostrobin could have directly induced conformational change on Asp75, in particular, or the catalytic triad region, in general. This, presumably, could disrupt the electron transfer process required for substrate binding at the active site, hence affecting the activity of the protease.

Studies have shown that the formation of low-barrier hydrogen bond between Asp and His (of the catalytic triad) facilitates the nucleophilic attack by the β-OH group of Ser on the acyl carbonyl group of substrates.[37–39] Besides Lys74, Leu149 might play a role toward the activity of pinostrobin in two ways. First, Leu149 could be blocking the entry of the ligand into the active site due to its position in the protease, as observed in Figure 5c,d. Second, Leu149 was seen to protrude toward the adjacent β-barrel which carried the residues Asp75 and His51. Erbel et al. (2006)[40] reported that the NS3 protease domain adopts a chymotrypsin-like fold with two β-barrels and that the catalytic triad is located at the cleft between the two β-barrels. Thus, upon binding Leu149 with pinostrobin, a conformational change of the residue could occur in order to reduce steric clashes, affecting the spatial conformation of the surrounding residues, in particular the catalytic triad. In conjunction with this, the electron transfer process involved between Asp75 and His51 might be affected, reducing the capability of the active site to bind to the substrate. This process could further increase the inhibition capability of pinostrobin.

Figure 5f shows the residues involved in hydrophobic interactions with pinostrobin, obtained by the Ligplot program. Besides the hydrophobic interactions, Trp83 also exhibited nonclassical hydrogen bonding interaction between the H atom on $N_{\epsilon 1}$ of its indole ring with the phenyl ring (B) of pinostrobin (Figure 5e). In this case of nonclassical hydrogen bonding, the hydrogen bond acceptor is the aromatic ring.[41] Brocchieri and Karlin (1994) reported that the interplanar angle (dihedral angle between the extended planes of interacting planar groups, α) between the phenyl ring of Phe and the aromatic ring of Trp to be favorable at $30° < \alpha < 90°$.[42] They also reported that, generally, planar interactions of Trp involved mostly the five-atom ring which is capable of forming a hydrogen bond (involving its imino group), engaging π-cloud electrostatic interactions, and also undergoing hydrophobic interactions. Electrostatic charges associated with the phenyl ring include a weak negative charge about the center of the aromatic ring and a weak positive charge projected at the ring pheriphery.[43] In this study, interactions were also observed between Trp83 and pinostrobin, where the bond distance between the H atom on $N_{\epsilon 1}$ of Trp83 and the center of the ring of the ligand ($R_{centroid}$) was 2.67 Å, and α was approximately 61.0°.

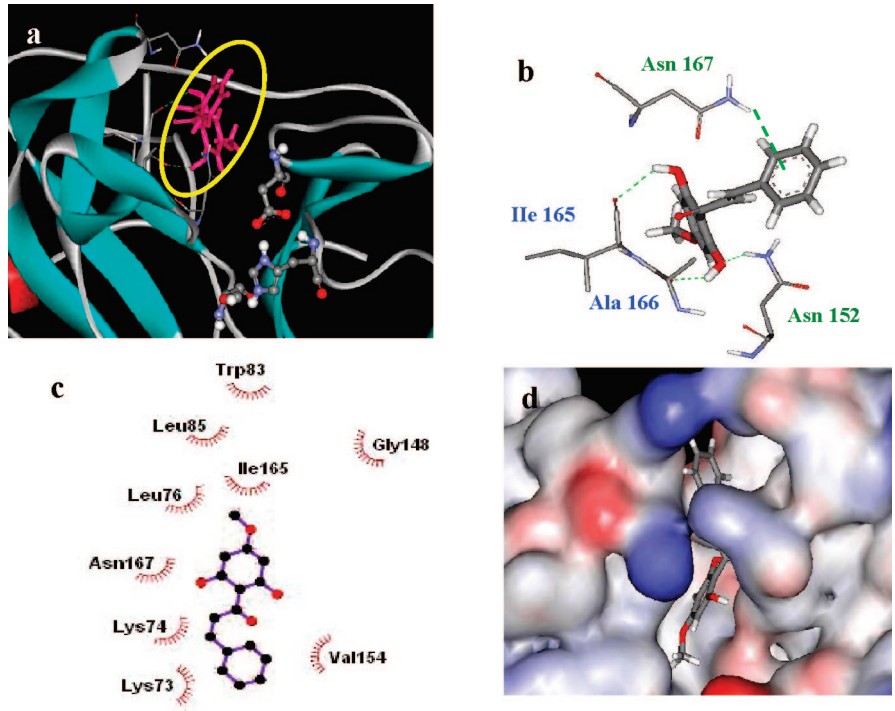

Figure 6. (**a**) View of pinostrobin chalcone (pink) at the binding site of Den2 protease (ribbons). Residues interacting with the ligand are shown as sticks. Catalytic triads are shown as balls and sticks. The yellow circle highlights the binding mode of the ligand which is confined to the C-terminal region of the protease, away from the catalytic triads. (**b**) Simplified view of pinostrobin chalcone interacting with surrounding residues. Residues labeled in green interact with the ligand via H-bonds, while those in blue exhibit both H-bond and van der Waals interactions. (**c**) 2D schematic diagram of residues in the binding site which exhibit hydrophobic interactions with pinostrobin chalcone obtained using the Ligplot program. Keys for the plot are the following: (blue ball-purple stick-black ball) ligand bond; (His51 with curved railroad-like ties) nonligand residue involved in hydrophobic contact; and (black ball with railroad-like ties) corresponding atom involved in hydrophobic contact. (**d**) Connolly surface representation of pinostrobin chalcone at the binding site nonligand residue involved in hydrophobic contact.

Pinostrobin Chalcone. Previous study had shown that pinostrobin chalcone did not exhibit inhibition activity (Table 1).[19] Investigation into the electrostatic interactions of pinostrobin chalcone with the binding site revealed that the surrounding amino acid residues of the protease involved in the interactions, via van der Waals and H-bond, were confined to the C-terminal region of the protease, with residues ranging from Asn152 to Asn167 (Figure 6a). This binding mode may not have any structural effect on the catalytic triad in promoting the disruption of electron transfer for the initiation of proteolytic processing. Presumably, binding activity of the ligand with its surrounding residues is confined to a region which may not impose any conformational change to the active site. Figure 6b illustrates the residues involved in H-bonding and van der Waals interactions with pinostrobin chalcone, in which a nonclassical H-bond is observed between Asn167 and the phenyl ring (B) of the ligand ($R_{centroid}$ = 3.64 Å, α = 40°). Figure 6c shows the residues involved in hydrophobic interactions with the ligand obtained from the Ligplot program. In addition to the interactions, the shape of the binding site was also complementary to the ligand's pose. From Figure 6d, observation of the hydrophobic pocket which accommodated the phenyl ring (B) of the ligand seemed to indicate that the ring was not placed directly in the center of the pocket, rather it was bent toward the left. This orientation may be attributed to the nonclassical H-bond interaction between the ring and Asn167.

The Other Ligands. Figure 7a−d shows the orientations of cardamonin, alpinetin, pinocembrin, and pinocembrin chalcone in the binding site of the protease, respectively. Except for pinocembrin chalcone, these ligands experienced H-bond and van der Waals interactions with almost the same surrounding residues. The common residues forming H-bond with the three ligands were Leu149 and Asn152. In addition, pinocembrin formed an additional H-bond with Val147 and Ile165. In terms of the van der Waals interactions, cardamonin interacted with Ile165, while alpinetin interacted with Val147 and Ile165, and pinocembrin with Asn167. Pinocembrin chalcone, however, did not demonstrate van der Waals interaction with any of the surrounding residues but interacted with Lys73 and Asn167 via H-bond.

The degree of inhibition offered by these four ligands was, in actual fact, similar to each other, even though both cardamonin and alpinetin exhibited slightly higher activities than pinocembrin chalcone and pinocembrin (Figure 2 and Table 1). The similarity in the degree of activities shown may be explained by the similar axis of orientation in the binding site (except for cardamonin; Figure 3) and similar mode of interactions as described above (except for pinocembrin chalcone; Figure 7). Unlike pinostrobin, these ligands did not form H-bond with Lys74, which may be the cause of the reduced activity observed when compared to pinostrobin. Nevertheless, Lys74 was involved in hydrophobic interaction with alpinetin, pinocembrin, and pinocembrin chalcone. Figure 8 illustrates the residues involved in hydrophobic interactions with the ligands using the Ligplot program. The observed activities of cardamonin, alpinetin, and pinocembrin could be due to the interactions of the ligands with Leu149, as shown in parts a, b, and d,

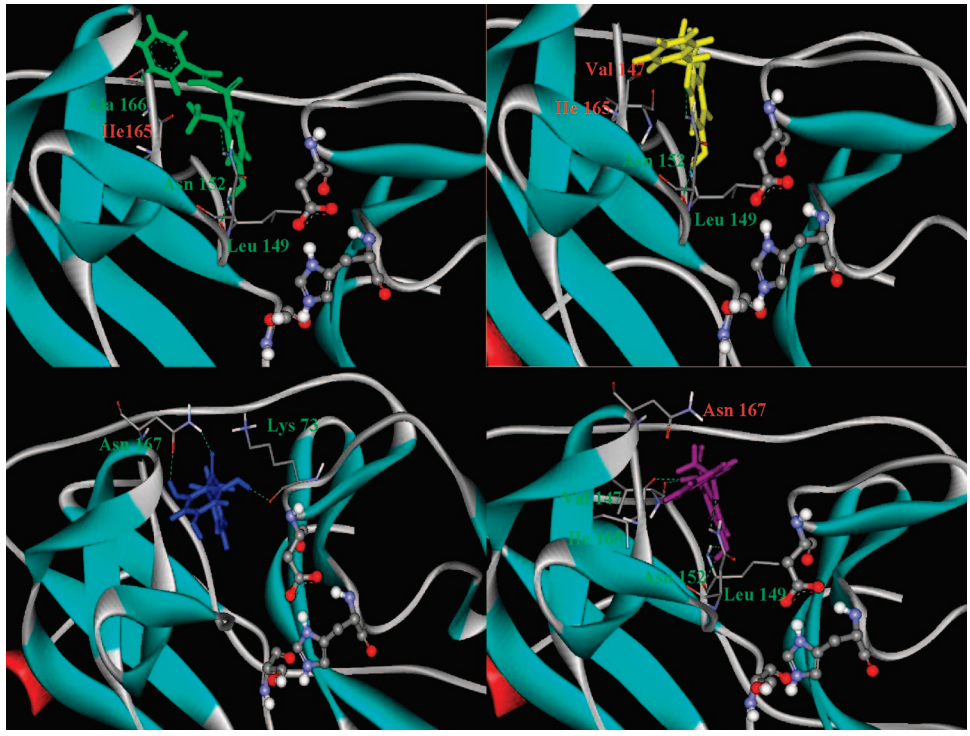

Figure 7. Models of ligands bound to the protease (ribbons) at the binding sites. The ligands shown are (**a**) cardamonin (green), (**b**) alpinetin (yellow), (**c**) pinocembrin chalcone (blue), and (**d**) pinocembrin (purple). Residues interacting with the ligands are shown as sticks. Catalytic triads are shown as balls and sticks. Residues labeled in green interact with the ligands via H-bonds, while those in red interact via van der Waals contacts.

respectively, of Figure 7. The effect of Leu149 on substrate-binding capability of the protease upon its binding with the ligands has been discussed earlier.

A different mode of interaction was observed with pinocembrin chalcone which did not bind to Leu149 to exhibit a similar inhibition effect. Rather, its H-bonding interaction with Lys73 could be the cause of the observed activity (Figure 7c). Lys73 is two residues downstream from Asp75, and interaction between the ligand with this residue may contribute directly to the conformational change of the active site, the extent of which, however, was not as great as that compared to the interaction between pinostrobin and Lys74. The fact that pinocembrin chalcone did not exhibit van der Waals interactions with the surrounding residues may be the cause for the lower activity seen in the pinocembrin chalcone than that of pinostrobin.

Structure−Activity Relationship (SAR) Analysis. The docking studies performed gave better structural insights and understanding on how the various ligands interacted with the protease in acting as noncompetitive inhibitors toward Den2 protease activity. Analysis of the structure−activity relationships of the ligands in this study may shed light on the important structure and conformation which could be applied in the design of new compounds.

This study affirmed that rigid conformation of the flavanones would ensure ligand activities. Opening up of the ring C, as found in the chalcones, would introduce higher flexibility to the ligands leading to a more extended conformation, thus requiring a different environment of the binding site (Figure 4). Higher flexibility of the chalcones also meant higher ΔG_{tor} compared to the corresponding flavanones and, hence, higher ΔG_{bind}. This would result in the chalcone binding being less favorable to the site when compared to the corresponding flavanones (Table 2). Pinocembrin showed the lowest values for the E_{dock} and ΔG_{bind}, followed by alpinetin and pinostrobin, indicating the parent structure of 7-hydroxyflavanone to have good binding capabilities with the protease.

The methoxy group at C7 on the ring A of pinostrobin may be important in creating the preferable electrostatic potential surface of the molecule in the 'search' for an optimal chemical environment within the binding site. In general, an electron-donating group at this position would be preferable for the design of new inhibitory compounds. The hydroxyl group at C5 on the ring A of pinostrobin could be considered to be an important pharmacophore. This hydroxyl group is very useful in forming H-bonds with the surrounding residues, particularly, between pinostrobin and Lys74 and between pinocembrin chalcone and Lys73 (the OH group is on C2′ of ring A for pinocembrin chalcone). For pinocembrin chalcone, the number of electrostatic interactions involved was the lowest among all the ligands reported. Thus, one might expect pinocembrin chalcone to exhibit a much lower inhibitory activity than the other ligands (except pinostrobin chalcone). However, from experiment, its activity was observed to be comparable to those of pinocembrin, cardamonin, and alpinetin. This could be attributed to its H-bonding interaction with Lys73 via the hydroxyl group, where Lys73 is positioned two residues downstream from Asp75. The conclusions derived from this study with regards to the importance of the methoxy and hydroxyl groups in determining the activity of the ligands are in accordance with those postulated by Tan (2005).[19]

The presence of the phenyl ring (B) in all the ligands is not of little importance and is essential in contributing to the hydrophobicity of the ligands. The entropic effects of

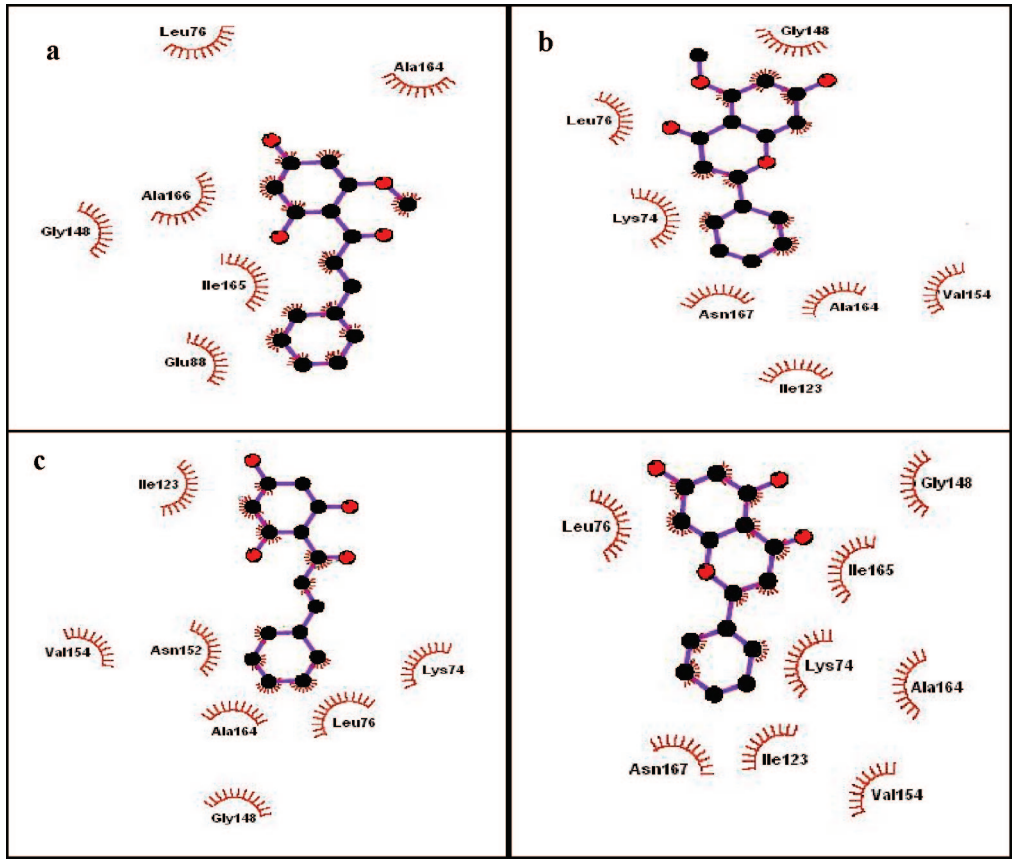

Figure 8. Schematic diagrams (2D) illustrating residues in the binding sites which are involved in hydrophobic interactions with (**a**) cardamonin, (**b**) alpinetin, (**c**) pinocembrin chalcone, and (**d**) pinocembrin. Keys for the plot are the following: (blue ball-purple stick-black ball) ligand bond; (His51 with curved railroad-like ties) nonligand residue involved in hydrophobic contact; and (black ball with railroad-like ties) corresponding atom involved in hydrophobic contact.

ligand binding vary with the degree of hydrophobic interactions in the system, contributing to the determination of the ΔG_{bind} value, and, as discussed earlier, the phenyl ring of pinostrobin and pinostrobin chalcone formed nonclassical H-bonding with Trp and Asn, respectively.

CONCLUSIONS

Three flavanones and three chalcones isolated from the plant *Boesenbergia rotunda* L. were docked onto the Den2 NS2B-NS3 protease using the AutoDock 3.0.5 software. Results obtained from this study are consistent with the experimental results illustrating the noncompetitive inhibitory activities for most of the ligands.[19] As expected, these ligands were found to bind to sites other than the active site of the Den2 serine protease. The calculated K_i values of these ligands were very small indicating that they bound considerably well to the allosteric binding site. The higher noncompetitive inhibitory activity shown by pinostrobin compared to the other compounds could be accounted for by H-bonding interaction with the backbone carbonyl of Lys74, which is bonded to Asp75 (one of the catalytic triad residues). This interaction was not observed with the other ligands. SAR analysis yielded some structural features which may be useful for the design of new compounds with potential inhibitory activities. These features are the rigid structure of flavanone, the C5 hydroxyl, and C7 methoxy groups on ring A and the phenyl ring (B).

Docking experiments were also performed with rigid ligands as well as with flexible ligands on the rigid protein structures (obtained from the PDB). To ensure that the observed interactions in the resulting structures were sustained, molecular dynamics calculations were often performed. Although molecular dynamics on the system was not carried out in the study, this additional technique could be carried out as a potential method of justification for the resulting structures. The results obtained did not illustrate any conformational changes that could occur after the ligand-protein binding process. To overcome such limitation, flexible-protein docking would be preferable. However, the development of computational strategies for this purpose is still in its infancy.[34] Several methods have been reported, and promising results have emerged from the application of combined methods such as the ensemble docking approach and an induced fit.[44]

Flexible-protein docking could be a way forward toward deeper insights into the present system which could aid in the design of new compounds for a therapeutic drug against dengue virus infections.

ACKNOWLEDGMENT

This work was supported in part by the Malaysian Ministry of Science, Technology and Innovation under the Top Down National Biotechnology Directory grant number 09-02-04-001BTK/TH/004 [UM 36-02-03-6008], the Academy of Science, Malaysia, under the Scientific Advancement Fund Allocation (SAGA 66-02-03-0049), and Universiti Malaya under the F-Vote grant number F0171/2005D.

REFERENCES AND NOTES

(1) Kautner, I.; Robinson, M. J.; Kuhnle, U. Dengue virus infection: epidemiology, pathogenesis, clinical presentation, diagnosis and prevention. *J. Pediatr.* **1997**, *131*, 516–524.

(2) Gubler, D. J. The global emergence/resurgence of arboviral diseases as public health problems. *Arch Med Res.* **2002**, *33*, 330–42. (WHO. 2007. http://www.who.int/csr/disease/dengue/impact/en/index.html (accessed May 20, 2008))

(3) Dengue kills 44 people in Malaysia, Sun Malaysia, 2007; May 20, 2007; http://story.malaysiasun.com/index.php/ct/9/cid/48cba686fe041718/id/250213/cs/1/ (accessed May 20, 2008).

(4) Irie, K.; Mohan, P. M.; Sasaguri, Y.; Putnak, R.; Padmanabhan, R. Sequence analysis of cloned dengue virus type 2 genome (New Guinea-C strain). *Gene* **1989**, *75*, 197–211.

(5) Falgout, B.; Pethel, M.; Zhang, Y. M.; Lai, C. J. Both nonstructural proteins NS2B and NS3 are required for the proteolytic processing of dengue virus nonstructural proteins. *J. Virol.* **1991**, *65*, 2467–2475.

(6) Yusof, R.; Clum, S.; Wetzel, M.; Murthy, H. M.; Padmanabhan, R. Purified NS2B-NS3 serineprotease of dengue virus type 2 exhibits cofactor NS2B dependence for cleavage of substrates with dibasic amino acids in vitro. *J. Biol. Chem.* **2000**, *275*, 9963–9969.

(7) Gorbalenya, A. E.; Donchenko, A. P.; Koonin, E. V.; Blinov, V. M. N-terminal domains of putative helicases of flavi- and pestiviruses may be serine proteases. *Nucleic Acids Res.* **1989**, *17*, 3889–3897.

(8) Bazan, J. F.; Fletterick, R. J. Detection of a trypsin-like serine protease domain in flaviviruses and pestiviruses. *Virology* **1989**, *171*, 637–639.

(9) Brinkworth, R. I.; Fairlie, D. P.; Leung, D.; Young, P. R. Homology model of the dengue 2 virus NS3 protease: putative interactions with both substrate and NS2B cofactor. *J. Gen. Virol.* **1999**, *80*, 1167–1177.

(10) Arias, C. F.; Preugschat, F.; Strauss, J. H. Dengue 2 virus NS2B and NS3 form a stable complex that can cleave NS3 within the helicase domain. *Virology* **1993**, *193*, 888–899.

(11) Clum, S.; Ebner, K. E.; Padmanabhan, R. Cotranslational membrane insertion of the serine proteinase precursor NS2B-NS3(Pro) of dengue virus type 2 is required for efficient in vitro processing and is mediated through the hydrophobic regions of NS2B. *J. Biol. Chem.* **1997**, *272*, 30715–30723.

(12) Tan, S. K.; Pippen, R.; Yusof, R.; Ibrahim, H.; Khalid, N.; Abd Rahman, N. Inhibitory activity of cycohexenyl chalcone derivatives and flavonoids of fingerroot, *Boesenbergia rotunda* (L.), towards dengue-2 virus NS3 protease. *Bioorg. Med. Chem. Lett.* **2006**, *16*, 3337–3340.

(13) Whitby, K.; Pierson, T. C.; Geiss, B.; Lane, K.; Engle, M.; Yi, Z.; Doms, R. W.; Diamond, M. S. Castanospermine, a potent inhibitor of Dengue virus infection in vitro and in vivo. *J. Virol.* **2005**, *79*, 8698–8706.

(14) Hrobowski, Y. M.; Garry, R. F.; Michael, S. F. Peptide inhibitors of dengue virus and West Nile virus infectivity. *Virol. J.* **2005**, *2*, 49.

(15) Putnak, J. R.; Coller, B.-A.; Voss, G.; Vaughn, D. W.; Clements, D.; Peters, I.; Bignami, G.; Hounga, H.-S.; Chena, R. C.-M.; Barvir, D. A.; Seriwatana, J.; Cayphas, S.; Garcon, N.; Gheysen, D.; Kanesa-thasan, N.; McDonell, M.; Humphreys, T.; Eckels, K. H.; Prieels, J.-P.; Innis, B. L. An evaluation of dengue type-2 inactivated, recombinant subunit, and live-attenuated vaccine candidates in the rhesus macaque model. *Vaccine* **2005**, *23*, 4442–4452.

(16) Yin, Z.; Patel, S. J.; Wang, W.-L.; Wang, G.; Chan, W.-L.; Ranga Rao, K. R.; Alam, J.; Jeyaraj, D. A.; Ngew, X.; Patel, V.; Beer, D.; Lim, S. P.; Vasudevan, S. G.; Keller, T. H. Peptide inhibitors of dengue virus NS3 protease. Part 1: Warhead. *Bioorg. Med. Chem. Lett.* **2006**, *16*, 36–39.

(17) Diamond, M. S.; Zachariah, M.; Harris, E. Mycophenolic acid inhibits dengue virus infection by preventing replication of viral RNA. *Virology* **2002**, *304*, 211–221.

(18) Ray, D.; Shi, P.-Y. Recent Advances in Flavivirus Antiviral Drug Discovery and Vaccine Development. *Recent Pat. Anti-Infective Drug Discovery* **2006**, *1*, 45–55.

(19) Tan, S. K. *Flavonoids from Boesenbergia rotunda (L). Mansf.: Chemistry, bioactivity and accumulation*; Ph.D. Thesis, Universiti Malaya, Kuala Lumpur 2005.

(20) Ibrahim, H.; Rahman, A. A. *Several ginger plants (Zingiberaceae) of potential value. In Malaysian Traditional Medicine: Proceedings of the Seminar on Malaysian Traditional Medicine*; Soepadmo, E., Goh, S. H., Wong, W. H., Din, L., Chuah, C. H., Eds.; Institute of Advanced Studies, University of Malaya, and Malaysian Institute of Chemistry: Kuala Lumpur, 1989; pp 159−161.

(21) Tuchinda, P.; Reutrakul, V.; Claeson, P.; Pongprayoon, U.; Sematong, T.; Santisuk, T.; Taylor, W. Anti-inflammatory cyclohexenyl chalcone derivative in Boesenbergia pandurata. *Phytochemistry* **2002**, *59*, 169–173.

(22) Tewtrakul, S.; Subhadhirasakul, S.; Kummee, S. HIV-1 protease inhibitory effects of medicinal plants used as self medication by AIDS patients. *Songklanakarin J. Sci. Technol.* **2003**, *25*, 239–243.

(23) Tewtrakul, S.; Subhadhirasakul, S.; Puripattanavong, J.; Panphadung, T. HIV-1 protease inhibitory substances from the rhizomes of *Boesenbergia pandurata* Holtt. *Songklanakarin J. Sci. Technol.* **2003**, *25*, 503–508.

(24) Friesner, R. A.; Bank, J. L.; Murphy, R. B.; Halgren, T. A.; Klicic, J. J.; Mainz, D. T.; Repasky, M. P.; Knoll, E. H.; Shaw, D. E.; Shelley, M.; Perry, J. K.; Francis, P.; Shenking, P. S. Glide: A New Approach for Rapid, Accurate Docking and Scoring. 1. Method and Assessment of Docking Accuracy. *J. Med. Chem.* **2004**, *47*, 1739–1749.

(25) Brown, M. J.; Henderson, D. E.; Hunt, C. Comparison of antioxidant properties of supercritical fluid extracts of herbs and the confirmation of pinocembrin as a principle antioxidant in Mexican oregano (Lippa gravolens). Electron. *J. Environ. Agric. Food Chem.* **2006**, *5*, 1265–1277.

(26) Jiang, R.-W.; He, Z.-D.; But, P. P.-H.; Chan, Y.-M.; Ma, S.-C.; Mak, T. C. W. A Novel 1:1 Complex of Potassium Mikanin-3-*O*-sulfate with Methanol. *Chem. Pharm. Bull.* **2001**, *49*, 1166–1169.

(27) Shoja, M. 5-Hydroxy-7-methoxyflavone. *Acta Crystallogr.* **1989**, *C45*, 828–829.

(28) Sanner, M. F. Python: A programming language for software integration and development. *J. Mol. Graphics Model.* **1999**, *17*, 57–61.

(29) Morris, G. M.; Goodsell, D. S.; Halliday, R. S.; Huey, R.; Hart, W. E.; Belew, R. K.; Olson, A. J. Automated Docking Using a Lamarckian Genetic Algorithm and an Empirical Binding Free Energy Function. *J. Comput. Chem.* **1998**, *19*, 1639–1662.

(30) Wallace, A. C.; Laskowski, R. A.; Thornton, J. M. LIGPLOT: a program to generate schematic diagrams of protein-ligand interactions. *Protein Eng.* **1995**, *8*, 127–134.

(31) McDonald, I. K.; Thornton, J. M. Satisfying hydrogen-bonding potential in proteins. *J. Mol. Biol.* **1994**, *238*, 777–793.

(32) National Cancer Institute, Developmental Therapeutics Program, Enhanced Database Browser. http://129.43.27.140/ncidb2/ (accessed May 20, 2008).

(33) Jorgensen, W. L.; Tirado-Rives, J. *Potential energy functions for atomic-level simulations of water and organic and biomolecular systems PNAS* **2005**, *102*, 6665–6670.

(34) Sousa, S. F.; Fernandes, P. A.; Ramos, M. J. Protein-Ligand Docking: Current Status and Future Challenges. *Proteins* **2006**, *65*, 15–26.

(35) Hetényi, C.; van der Spoel, D. Efficient docking of peptides to proteins without prior knowledge of the binding site. *Protein Sci.* **2002**, *11*, 1729–1737.

(36) Kitchen, D. B.; Decornez, H.; Furr, J. R.; Bajorath, J. Docking and scoring in virtual screening for drug discovery: Methods and application. *Nature Rev. Drug Discovery* **2004**, *3*, 935–949.

(37) Frey, P. A.; Whitt, S. A.; Tobin, J. B. A Low-Barrier Hydrogen Bond in the Catalytic Triad of Serine Proteases. *Science* **1994**, *264*, 1927–1930.

(38) Santis, L. D.; Carloni, P. Serine Proteases: An Ab Initio Molecular Dynamics Study. *Proteins* **1999**, *37*, 611–618.

(39) Hunkapiller, M. W.; Forgac, M. D.; Richards, J. H. Mechanism of Action of Serine Proteases: Tetrahedral Intermediate and Concerted Proton Transfer. *Biochemistry* **1976**, *15*, 5581.

(40) Erbel, P.; Schiering, N.; D'Arcy, A.; Renatus, M.; Kroemer, M.; Lim, S. P.; Yin, Z.; Keller, T. H.; Vasudevan, S. G.; Hommel, U. Structural basis for the activation of flaviviral NS3 proteases from dengue and West Nile virus. *Nat. Struct. Mol. Biol.* **2006**, *13*, 372–373.

(41) Gervasio, F. L.; Chelli, R.; Procacci, P.; Schettino, V. The Nature of Intermolecular Interactions between Aromatic Amino Acid Residues. *Proteins* **2002**, *48*, 117–125.

(42) Brocchieri, L.; Karlin, S. Geometry of interplanar residue contacts in protein structures. *Proc. Natl. Acad. Sci. U.S.A.* **1994**, *91*, 9297–9301.

(43) Burley, S. K.; Petsko, G. A. Weakly polar interactions in proteins. *Adv. Protein Chem.* **1988**, *39*, 125–189.

(44) Cavasotto, C. N.; Kovacs, J. A.; Abagyan, R. A. Representing Receptor Flexibility in Ligand Docking through Relevant Normal Modes. *J. Am. Chem. Soc.* **2005**, *127*, 9632–9640.

CI700388K